NATIONAL AERONAUTICS AND SPACE ADMINISTRATION

Technical Report 32-1178

The Effect of Injector-Element Scale on the Mixing and Combustion of Nitrogen Tetroxide-Hydrazine Propellants

David D. Evans
Howard B. Stanford
Robert W. Riebling

JET PROPULSION LABORATORY
CALIFORNIA INSTITUTE OF TECHNOLOGY
PASADENA, CALIFORNIA

November 1, 1967

NATIONAL AERONAUTICS AND SPACE ADMINISTRATION

29b JPL Technical Report 32-1178 END

3 The Effect of Injector-Element Scale on the Mixing and Combustion of Nitrogen Tetroxide-Hydrazine Propellants 6

6 David D. Evans
Howard B. Stanford
Robert W. Riebling 9

Approved by:

D. Dipprey

D. Dipprey, Manager
Liquid Propulsion Section

1 JET PROPULSION LABORATORY
CALIFORNIA INSTITUTE OF TECHNOLOGY
PASADENA, CALIFORNIA 3

9 November 1, 1967 10CV

TECHNICAL REPORT 32-1178

Prepared Under Contract No. NAS 7-100
National Aeronautics & Space Administration

25

Contents

Tables

Contents (contd)

Tables (contd)

Figures

Abstract

The effect of injector element physical size on the mixing of unlike-impinging doublet streams of nitrogen tetroxide and hydrazine at 150 psia chamber pressure was investigated. Single impinging-jet and impinging-sheet elements of 10-, 100-, and 2000-lbf thrust were fired in a series of experiments designed to measure their degree of separation into fuel-rich and oxidizer-rich combustion zones in the resulting reactive sprays. At this chamber pressure, very poor mixing was found at the 2000-lbf level of thrust per element for both the jets and the sheets; at 100-lbf the jets "blew apart" due to combustion effects, but the sheets did not; and neither jets nor sheets separated at the 10-lbf thrust scale. These results are attributed to rapid liquid-phase combustion reactions between the hypergolic propellants at the impingement interface, which can effectively blow apart the two streams and prevent their efficient mixing and combustion. The severity of these combustion effects increases with the physical size of the injection elements, but the mixing process is less prone to disruption when flat sheets are used. The results indicate that mixing data obtained in nonreactive spray tests must be used with caution in the design of injectors for high levels of thrust per element.

The Effect of Injector-Element Scale on the Mixing and Combustion of Nitrogen Tetroxide-Hydrazine Propellants

I. Introduction

For most propellant combinations, several primary processes must be accomplished efficiently to ensure efficient combustion, regardless of the type of injector employed; these are: (1) propellant mixing, (2) atomization and vaporization, and (3) chemical reaction. Normally, chemical reaction rates are quite rapid compared with the rates of mixing and atomization, so that one or both of the latter two physical processes usually controls the overall combustion rate.

Unlike-doublet-injection elements, which are used in many liquid bipropellant rocket-engine injectors, depend for both primary mixing and atomization on the impingement of a pair of unlike propellant streams. Historically these streams have been round jets, although in recent years the use of flat-sheet doublet elements has also been explored at JPL (Ref. 1). In either case, the phenomena occurring in the impingement region determine the degrees of mixing and atomization that can be realized and therefore, to a large extent, the combustion efficiency. Anything that interferes with, or disrupts, this impingement process would be expected to impair propellant mixing and atomization and, thus, degrade performance. Propellant streams that misimpinge or miss each other entirely are two common examples.

Elverum and Staudhammer (Ref. 2) noted yet another impingement-disrupting phenomenon in photographic studies of open flames resulting from unlike impingement of jets of nitrogen tetroxide (N_2O_4) and hydrazine (N_2H_4). They found that jets of those two hypergolic liquids reacted very rapidly on contact, with immediate and violent evolution of gases at the impingement interface. This reaction appeared to blow apart, or separate, substantial portions of the fuel and oxidizer streams before normal liquid-phase mixing and atomization had had time to occur. The coloration of the resulting flames (Fig. 1a) indicated that they were fuel-rich on one side and oxidizer-rich on the other.

Johnson (Ref. 3) verified quantitatively what Elverum and Staudhammer had observed visually. In a series of 2000- lbf thrust rocket-motor firing experiments designed to detect and measure the extent of stream separation, Johnson found that combustion effects in the impingement region disrupted the normal exchange of momentum between the two jets of an unlike doublet element with various hypergolic liquid-propellant combinations.

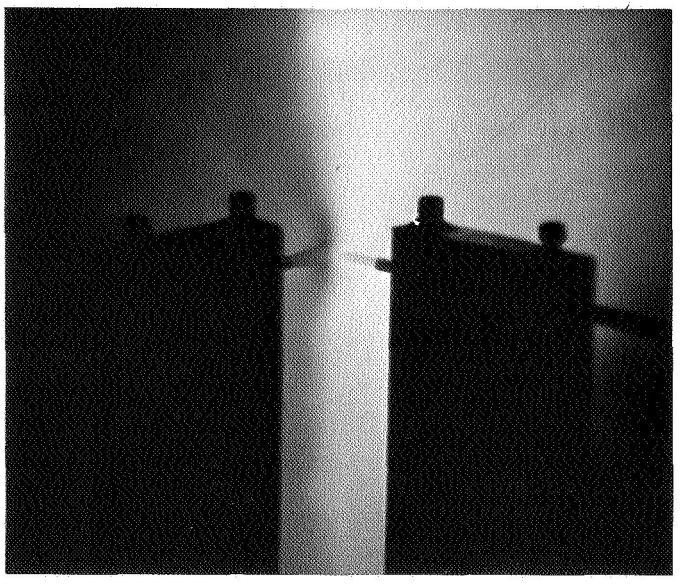

Fig. 1a. N_2O_4 stream impinging on N_2H_4 stream, showing separation

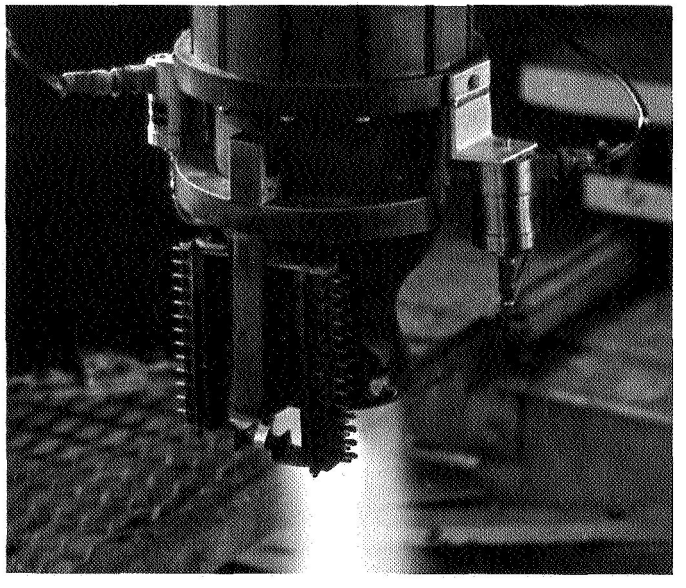

Fig. 1b. Visual evidence of stream separation with 2000-lbf single-element impinging-sheet injector (no side sprays)

However, stream separation was *not* noted in tests with nonhypergolic propellants. The jets used in his experiment were relatively large (0.236-in. diameter).

In succeeding years, Johnson's basic work was extended by other investigators, who studied the effects of the size and kind of injection element on the stream

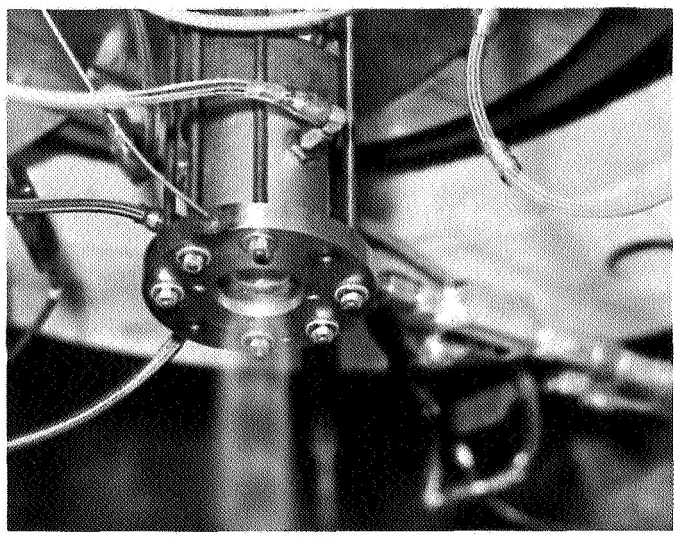

Fig. 1c. Apparent lack of major-stream separation with 100-lbf single-element impinging-sheet injector (no side sprays)

separation phenomenon, with particular attention to the N_2O_4/N_2H_4 propellant combination. This report presents and analyzes their results.

II. Experimental Procedure

Several sizes and two basic types of injector elements were studied. To determine if stream separation were, in fact, taking place, each injector was fired in a specially constructed thrust chamber, such as is shown schematically in Fig. 2. Three different sizes of chambers were used —and these are described in detail in the Section IV of of this report—but the following discussion applies to all the thrust chambers.

The combustion chambers were divided into two longitudinal channels by a baffle plate oriented in a plane perpendicular to the injector face. The top of this baffle was situated far enough from the injector to avoid interference with the impingement process, and the plate extended to a point in the convergent portion of the nozzle just upstream of the physical throat. Two full-cone, commercial spray nozzles were located in the chamber wall, one on each side of the baffle; and in the 10- and 100-lbf firings, turbulence rings were mounted in the chamber, downstream of the spray nozzles.

The experiments consisted of determining the difference in performance measured when the propellants sprayed from the side nozzles—one spraying fuel and the other oxidizer—were reversed. The concept involved is

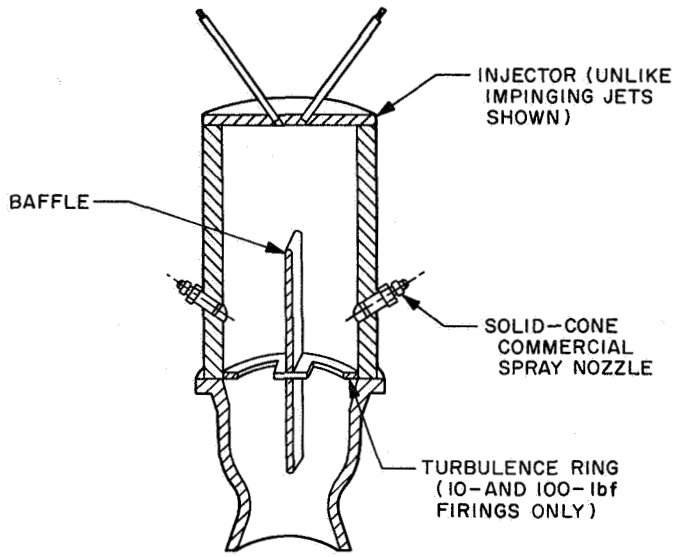

Fig. 2. Schematic representation of baffled thrust chambers used for evaluating combustion effects

that, if the propellants flowing from the main injector are repelled from each other to form a fuel-rich zone on the fuel orifice side and an oxidizer-rich zone on the oxidizer-orifice side of the chamber, the baffle should prevent secondary mixing from turbulence and diffusion. Thus, one channel should contain an oxidizer-rich flow and the other a fuel-rich flow of gases. Spraying oxidizer into fuel-rich gases and fuel into the oxidizer-rich gases (termed *unlike* propellants, henceforth), should increase performance, while spraying fuel into fuel-rich gases and oxidizer into oxidizer-rich gases (termed *like* propellants, henceforth) should reduce performance. If the streams from the main injector do not blow apart, and a relatively uniform mixture ratio distribution exists in the chamber, performance should remain relatively unchanged when the propellant sprays are reversed. If the streams penetrate through each other, the fuel-rich and oxidizer-rich channels will be reversed, and the performance changes should indicate this condition also.

To minimize the variables, the main-element flow rates were maintained essentially constant within each series of tests. The side-flow rates from the spray nozzles were varied to maintain a constant overall mixture ratio of approximately 1.2. The amount of side flow needed to maximize performance was an indication of the degree of mixture ratio maldistribution resulting from disturbances in the impingement region.

III. Chronology

It is important to bear in mind that the results reported herein were obtained from several different research programs, conducted by various individuals at different times. For this reason, there is more disparity in the hardware and propellant flow-control configurations than would be expected for a single, continuous study. Such disparities do not interfere with the validity of the experiments or the conclusions drawn from them, but in some cases they do make it impossible to compare and order, on an equal basis, the performance efficiencies delivered by the various kinds and sizes of injectors.

The studies that form the subject of this report were conducted over approximately a four-year period, in the following chronological order. The first stream separation experiments were made by Johnson (Ref. 3) who studied 2000-lbf single elements comprising both impinging jets and impinging sheets. The impinging-sheet injector used in this work was a very early model that featured both rounded deflectors and an extremely wide separation, or spacing, between the deflectors. Subsequent work by Evans (Ref. 4) led to the adoption of square-edged deflectors with close spacing as the standard impinging-sheet configuration because of their demonstrated higher combustion efficiencies. Therefore, Johnson's impinging-sheet results are now considered as being not representative of the behavior of presently- accepted impinging-sheet injection elements, and are not included in this report. His impinging-jet work is, however, pertinent, and will be presented again and discussed in a later section.

Stanford (Ref. 5) then studied stream separation with 100-lbf single-element impinging-jet and impinging-sheet injectors. His 100-lbf impinging-sheet injector was, likewise, one of the early versions now considered to be nonrepresentative, so only his impinging-jet results are reported and discussed here.

Still later, Stanford investigated 10-lbf single-element injectors using both jets and sheets (Ref. 6). By this time, however, the results of Evans' work were available, and the 10-lbf impinging-sheet injector used by Stanford was typical of contemporary designs. Accordingly, both the 10-lbf jet and sheet results are reported and discussed here.

Finally, Riebling (Refs. 7 and 8) built updated versions of the 2000- and the 100-lbf impinging-sheet injectors, and repeated the earlier stream-separation experiments with them. Thrust-chamber modifications in the interim prevented evaluation of these two newer injectors in exactly the same chamber geometry used earlier.

Similar remarks pertain to the layout of the various flow control systems (see Section IV-C) because firings

were conducted at both the Pasadena and Edwards Test Station facilities over the 4-yr period.

IV. Apparatus

A. Injectors

Two kinds of unlike-impinging-doublet elements were used—impinging jets and impinging sheets. All injectors were single elements, constructed of stainless steel. For convenience, they will be referred to in this report in terms of their nominal vacuum thrust per element at $\epsilon = 40{:}1$ with the N_2O_4/N_2H_4 propellant combination at a mixture ratio (oxidizer to fuel) of 1.2 and a chamber pressure of 150 psia. Because of the general familiarity of impinging-jet injectors, relatively little space will be devoted to describing their design and functioning. Impinging-sheet injectors, at least the kind used in these studies, are somewhat novel, and their configuration will be discussed in greater detail.

The salient features of the impinging-jet injectors are summarized in Table 1. Fuel and oxidizer orifice diameters were identical, a condition that results in both

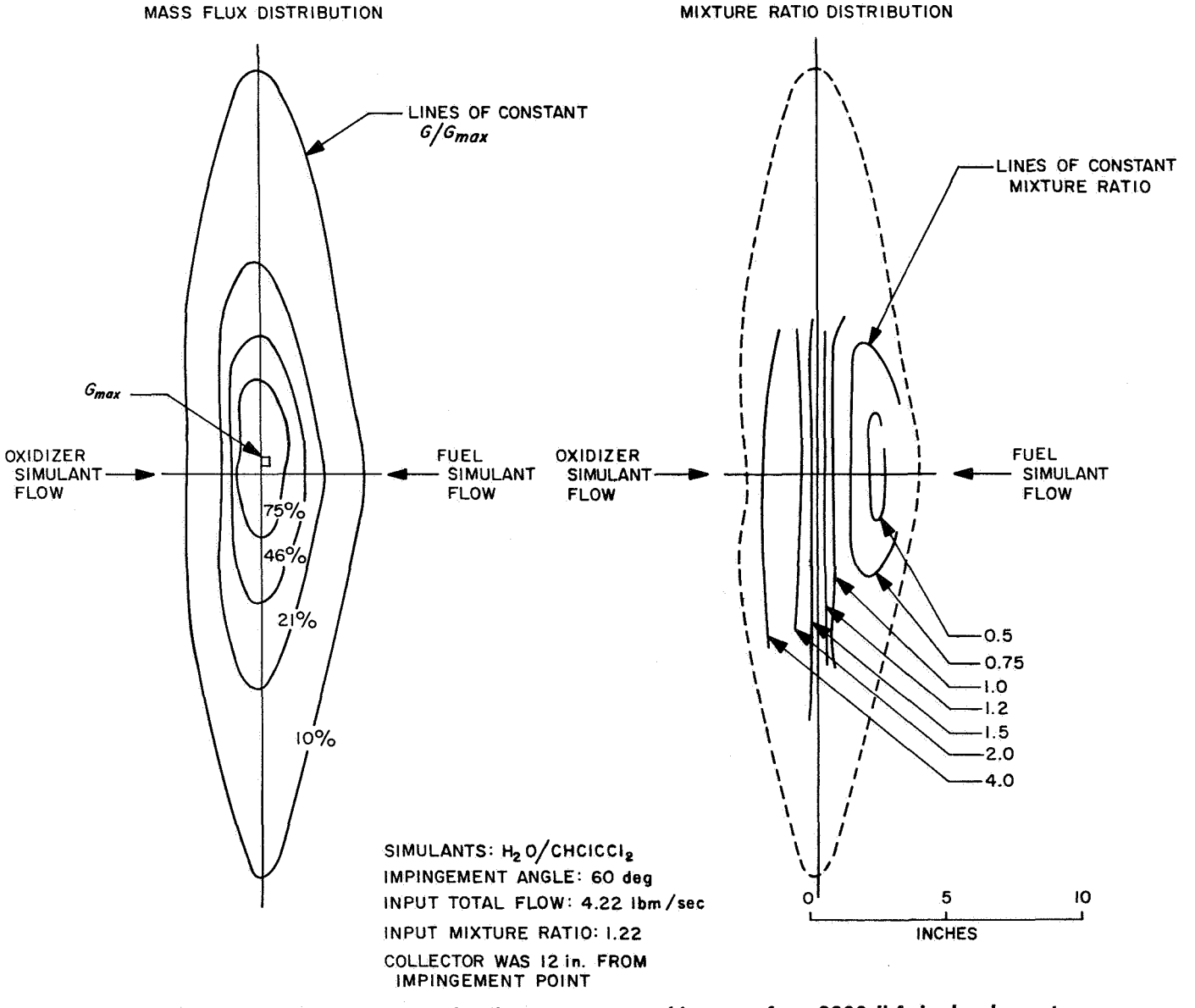

Fig. 3. Mass and mixture ratio distributions measured in spray from 2000-lbf single-element impinging-jet injector under nonreactive conditions

Table 1. Summary of impinging-jet injector geometry

Nominal thrust, lbf	Orifice diameter, in.	Orifice length, diameters
2000	0.236	50
100	0.064	100
10	0.022	100

equal-stream momenta and equal injection-pressure drops with N_2O_4/N_2H_4 propellants at a mixture ratio of 1.2. The jets were formed, in each case, from long orifice tubes to assure the attainment of fully-developed turbulent flow with its characteristic and reproducible hydraulic characteristics. In addition, meticulous care was taken to ensure that the orifice exits were sharp-edged, free of burrs, and as nearly round as possible, and that the jet centerlines intersected at the impingement point. The three sizes of impinging-jet element were geometrically similar, in that each had an impingement angle of 60 deg and the free-jet length (between the orifice exit and the impingement point) was equal to four jet diameters.

The nonreactive mass and mixture ratio distributions measured in the spray produced by the 2000-lbf single-element impinging-jet injector are shown in Fig. 3. These are typical of the distributions found for the other two injector sizes, and for properly constructed impinging-jet elements, in general. Mass flux is distributed nearly symmetrically about the spray axis, and mixture ratio varies continuously from fuel-simulant-rich conditions on the oxidizer-simulant side to oxidizer-simulant-rich conditions on the fuel-simulant side, indicating interpenetration of the two nonreactive jets.

A typical impinging-sheet injection element is shown in Fig. 4. Jets of liquid from the round orifice tubes are directed tangentially[1] against a solid, concave deflector surface, where they are spread and flattened into very thin flowing sheets (Ref. 9). Formed separately, the sheets are then brought together along an impingement line. The configuration and nomenclature of a typical sheet-formation device are shown schematically in Fig. 5. The deflector is a concave cylindrical surface of radius R and included angle θ, fed tangentially by an orifice of inside diameter d. An additional and most useful parameter is termed the *overhang* h, described by

$$h = R\,(1 - \cos\theta) \qquad (1)$$

[1]This device should not be confused with so-called *splash plate* injectors, which characteristically impinge fuel and oxidizer, either singly or in combination, in a *non-tangential* manner against some solid surface, where considerable splashing or splattering is intended to take place.

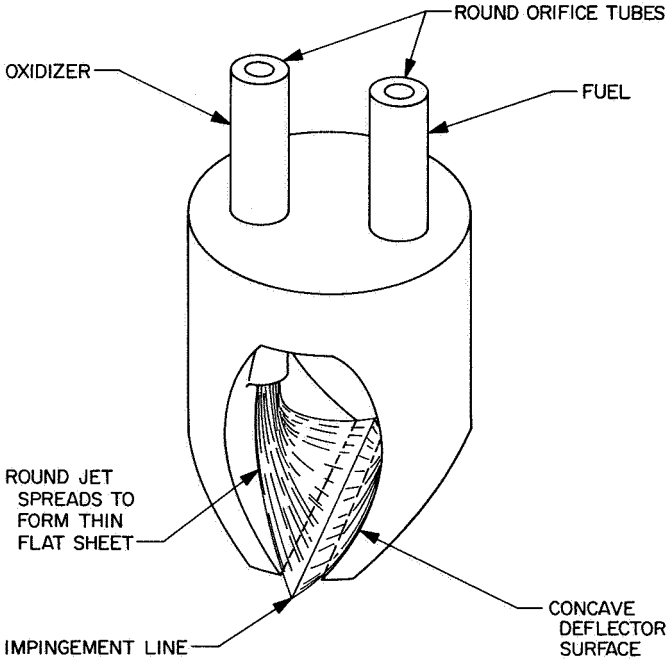

Fig. 4. Typical impinging-sheet injection element

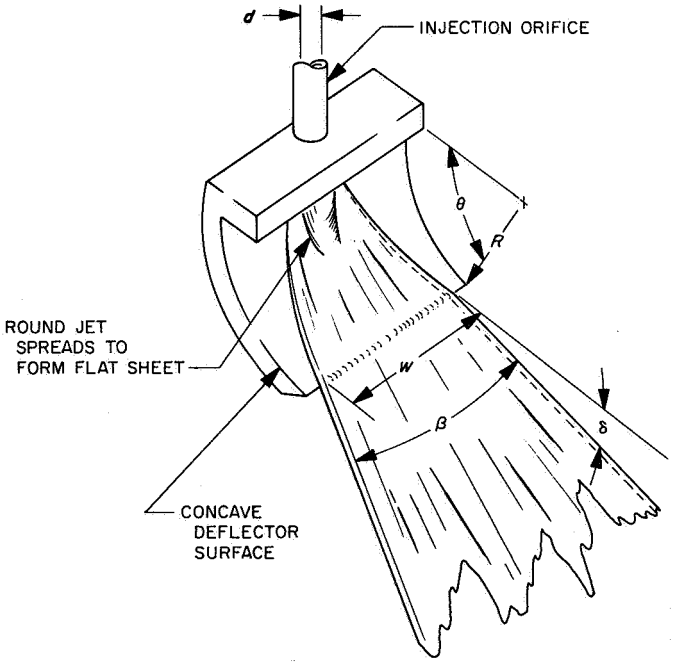

Fig. 5. Configuration and nomenclature of typical sheet-formation device

which is the transverse distance to which the deflector protrudes into the otherwise undisturbed round jet (Ref. 9).

The key dimensions of the impinging-sheet injection elements used in the present experiments are summarized in Table 2. As in the case of the impinging-jet injectors, the orifices were long, straight tubes of equal area, aligned to assure true tangential introduction of the jets onto the deflectors. The latter had surface finishes of 64 μin. (rms) or better, and the knife-edges were separated by the deflector spacings shown in Table 2. The sheets impinged at an angle of 90 deg in each case. The approximate sheet thicknesses reported in Table 2 were estimated from the generalized sheet thickness correlation of Ref. 9. Figure 6 is a photograph of the 2000-lbf thrust impinging-sheet element.

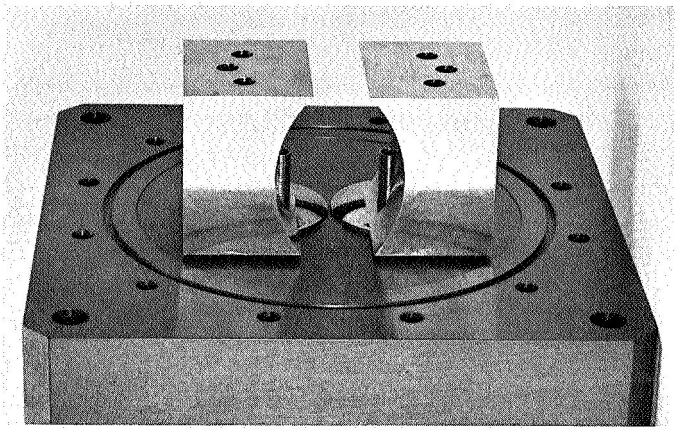

Fig. 6. 2000-lbf single-element impinging-sheet injector

The nonreactive mass and mixture ratio distributions measured in the spray produced by the 2000-lbf single-element impinging-sheet injector are shown in Fig. 7. These are typical of the distributions found with the 100-lbf element, and with 10- and 25-lbf elements studied in other programs. The distributions are quite similar to those found for impinging-jet elements (Fig. 3) and indicate sheet penetration in the absence of combustion effects.

B. Thrust Chambers

All three thrust chambers were heavy-weight, uncooled models, similar to the one shown schematically in Fig. 2; they differed mainly in physical size and the mechanical details of construction. Table 3 lists the key dimensions

Table 2. Summary of impinging-sheet injector geometry

Injector nominal thrust, lbf	Orifice diameter, in.	Orifice length, diameters	Deflector radius, in.	Deflector angle, deg	Deflector overhang ratio h/d, dimensionless	Deflector spacing, in.	Approximate maximum sheet thickness, in.
2000	0.325	100	2.330	45	2.07	0.10	0.05
100	0.075	100	0.580	45	2.27	0.05	0.01
10	0.018	100	0.160	45	2.60	0.05	0.002

Table 3. Summary of thrust-chamber geometry

Nominal thrust level, lbf	Injector type	Throat area, in.^{2}	Contraction area ratio ϵ_c	Expansion area ratio ϵ_e	Characteristic length L^*, in.	Convergence half-angle, deg	Divergence half-angle, deg
2000[a]	Jets	6.07[b]	5.65[b]	5.02[b]	187[b]	22.5	22.5
2000[a]	Sheets	6.07[b]	5.65[b]	3.06[b]	187[b]	22.5	22.5
100	Jets	0.544	5.65	2.70	50	30	15
100	Sheets	0.544	5.65	2.70	38.5	30	15
10	Jets and sheets	0.0385	5.65	2.70	20	30	15

[a]Neither of the 2000-lbf thrust chambers had a turbulence ring.

[b]Calculated by accounting for the baffle, with a cross-sectional area of 1.562 in.^{2}, which extended to the plane of the physical throat in the 2000-lbf chamber. In the 10- and 100-lbf chambers, the baffles extended only as far as a contraction ratio of 2.0, so their areas were not subtracted from the open-throat areas.

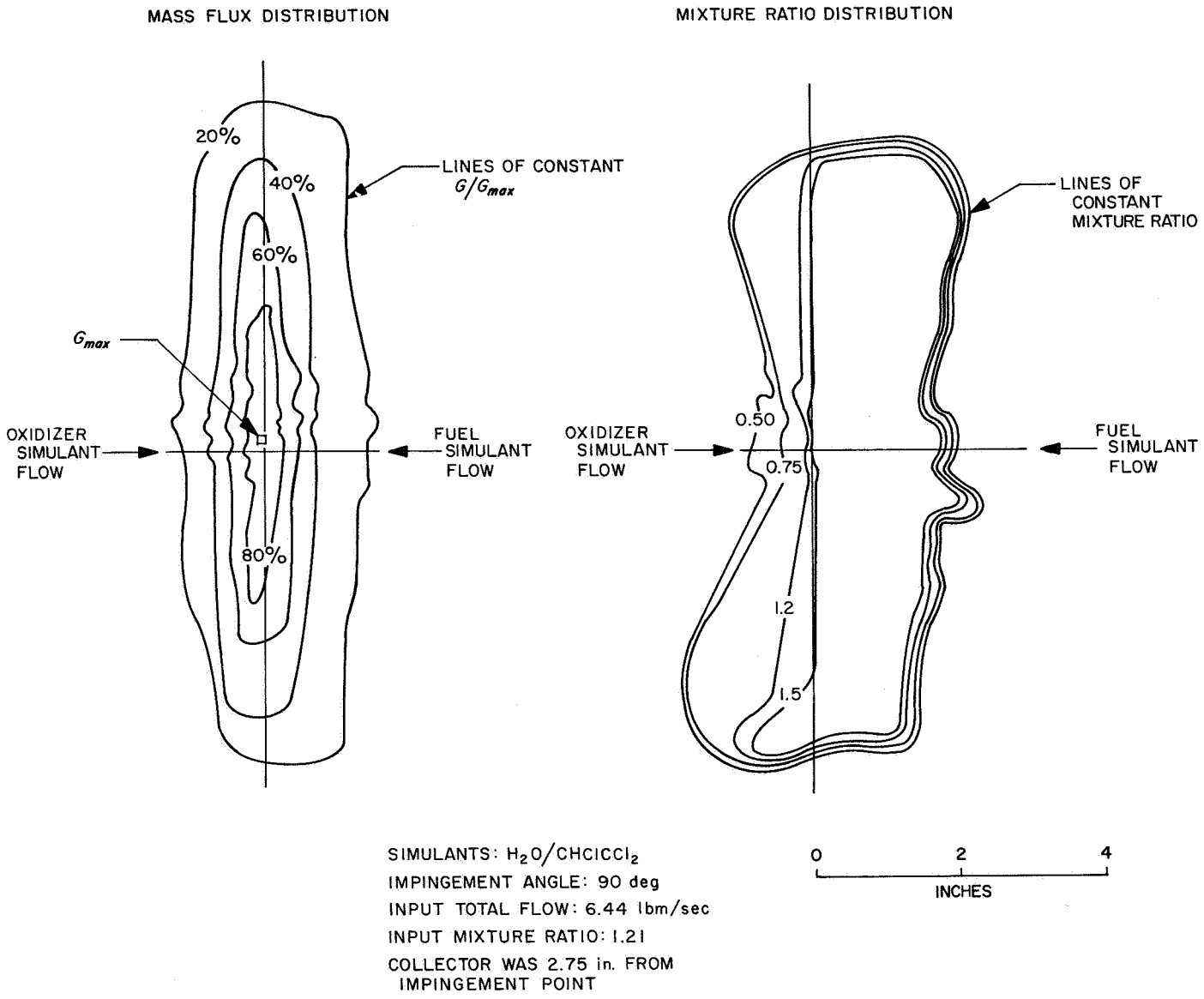

Fig. 7. Mass and mixture ratio distributions measured in spray from 2000-lbf single-element impinging-sheet injector under nonreactive conditions

of each chamber. The original 10- and 100-lbf chambers were linearly scaled-down versions of the 2000-lbf model; all three, therefore, had the same contraction-area ratio and ratio of cylindrical length to chamber diameter (4.15). This method of scaling, together with the fact that the 100-lbf impinging-sheet injector was fired in a somewhat shorter chamber than the 100-lbf impinging-jet injector, resulted in widely different values of the characteristic length L^*, as shown in Table 3. However, L^* was not considered to be of fundamental importance to the experiment, since relative changes in c^* efficiency, not absolute values, were taken as the measure of combustion effects. Furthermore, the performance obtained at one characteristic length was not to be compared with that obtained at any other.

The expansion-area ratio and the conical half-angles for the 2000-lbf chamber differed from those for the other two chambers because, in an effort to conserve program costs, an existing nozzle having these dimensions was employed. It was fired at its original expansion area ratio of 5.02 in the impinging jet tests but had been cut back to 3.06 by the time the impinging-sheet firings were made; the cutback was done to minimize the possibility

of exhaust-jet separation during an interim program using this nozzle.

The baffle plates were supported within the chambers by means of turbulence rings with a total open area equal to 2½ times the throat area. The original design called for each baffle plate to extend as far as the plane of the physical throat. However, serious erosion of the baffles occurred in early tests with the 10- and 100-lbf engines; their baffles were subsequently cut back so they terminated at a 2-to-1 contraction area ratio, which resulted in satisfactory operation. The baffles and turbulence rings were made of mild steel for the 2000- and 100-lbf engines, and of pyrolytic graphite for the 10-lbf engine. Figure 8 is an exploded view of the 10-lbf apparatus.

C. Flow Control

The flow of propellants was controlled by solenoid valves for all three engine sizes. Side flows were introduced into the chamber through solid-cone commercial spray nozzles, with in-line restrictors to maintain the desired low rates of flow.

Several different methods of determining the various flow rates were used, depending on both the engine scale

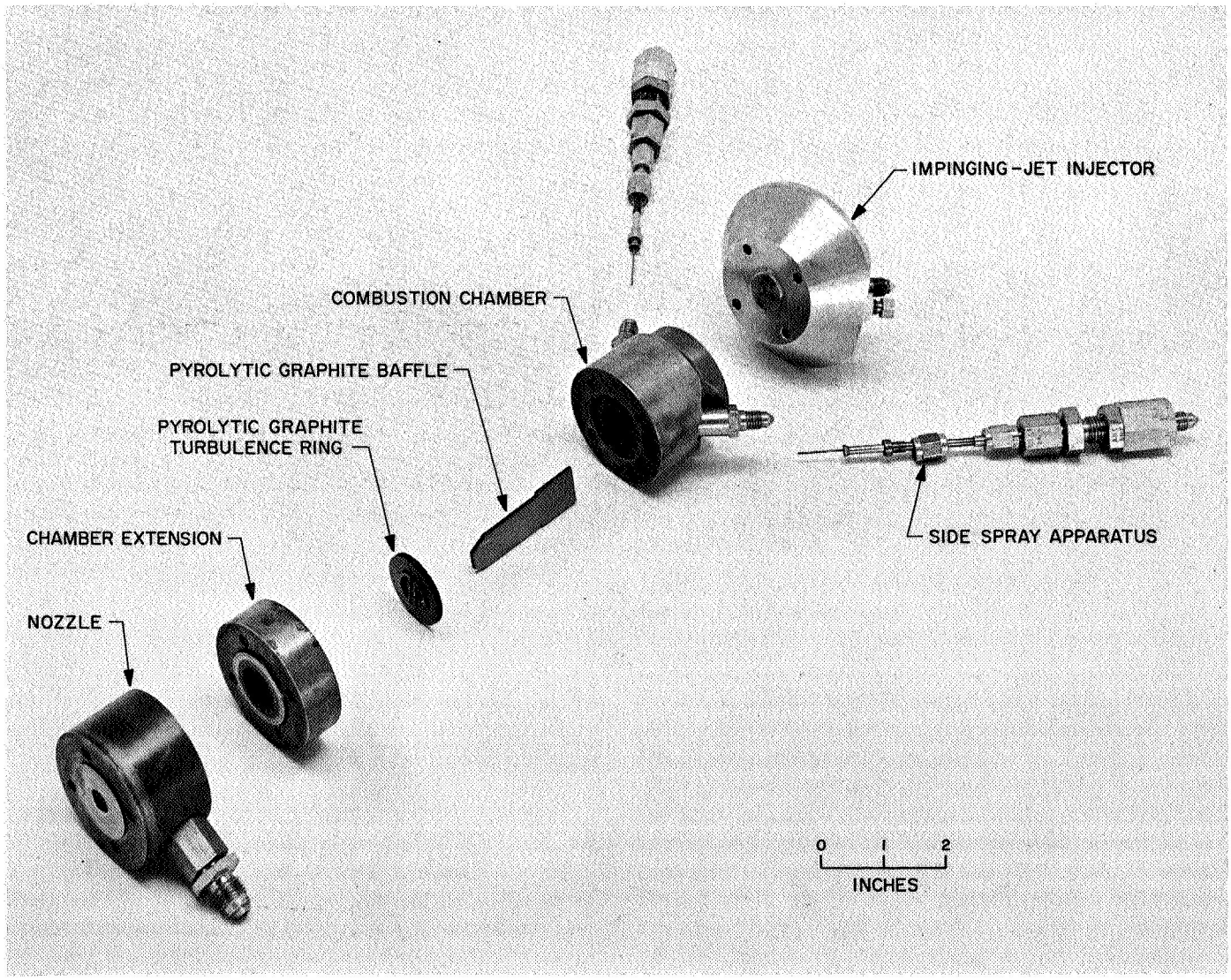

Fig. 8. Exploded view of 10-lbf engine assembly

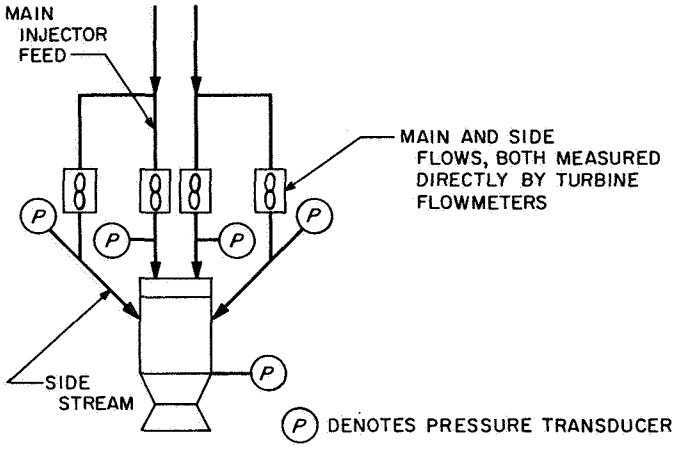

Fig. 9. Schematic flow diagram of flow-control system for 2000-lbf impinging-jet, and 2000-lbf and 100-lbf impinging-sheet experiments

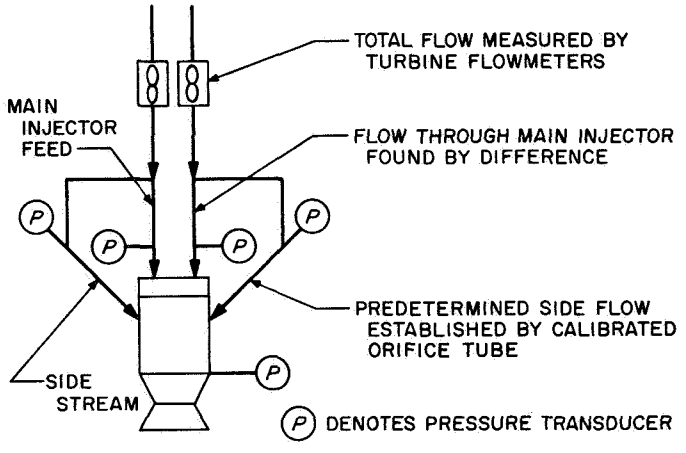

Fig. 10. Schematic flow diagram of flow-control system for 100-lbf impinging-jet experiments

and the availability of instrumentation at the test facilities. These are shown schematically in Figs. 9 through 11. Both the main and side stream flows were measured directly with in-line turbine flowmeters in the 2000-lbf impinging-jet and impinging-sheet, and in the 100-lbf impinging-sheet experiments (Fig. 9). However, in the 100-lbf impinging-jet firings, which were made at a different facility, side flows were metered into the chamber by calibrated orifice tubes because of the nonavailability of suitable flow meters to measure the small flows (Fig. 10). The total flow to the engine was measured with flow meters and the flow to the main injector was determined by difference. The same procedure was followed for the 10-lbf impinging-jet firings (Fig. 11), except that the total flow to the engine was measured by means of orifice meters and differential pressure transducers.

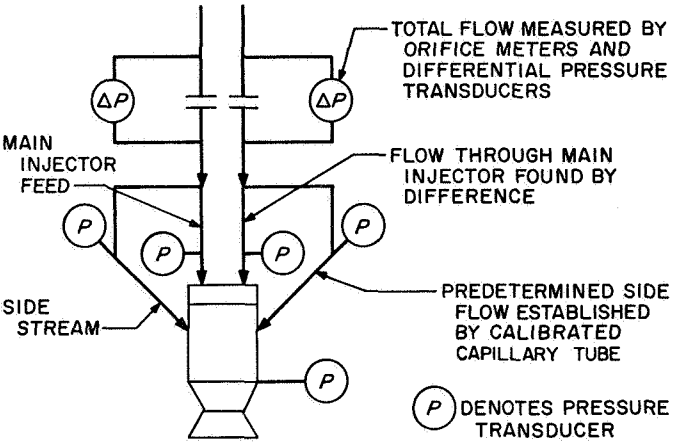

Fig. 11. Schematic flow diagram of flow-control system for 10-lbf impinging-jet and impinging-sheet experiments

The valve timing and hydraulic lags were such that the side flows typically attained steady-state about 0.5 sec after the main injector flows did. Mild purges through the spray nozzles prevented entry of propellants from the main injector before the start of side flow. All propellant lines were purged with gaseous nitrogen at the conclusion of each test.

The 10- and 100-lbf impinging-jet injectors were designed so that the side flows could also be introduced at the injector face, as an alternative to introducing them into the chamber. The flow-control systems for injector-end side-spray injection were identical to those just described, with the chamber ports being plugged when not in use. As will be seen in Section V, the location of the side-spray apparatus had little effect on performance, so for the sake of simplicity only chamber side flows were used in the majority of experiments.

V. Results

Experimental results for the 2000-lbf impinging-jet injector firings are reported in Ref. 3. Tables 4 through 9 summarize the results of the remainder of the stream separation experiments. The firing durations were nominally 3 to 5 sec in each case. The chamber pressures reported are stagnation values, obtained from static pressures measured near the entrance to the convergent section of the nozzle by application of the standard correction. Characteristic velocities were calculated on the basis of the *total* flowrate $\dot{w}_t$ of propellants injected into the chamber. The weight percent side flow in each case is the sum of the fuel and oxidizer side flows ($\dot{w}_{o_s}$ and

Table 4. Results of baffled-chamber firings to determine degree of stream separation of unlike impinging sheets in 2000-lbf injector (chamber side spray)

Test No.	Kind of side spray	Oxidizer flow, lbm/sec		Fuel flow, lbm/sec		Total flow $\dot{w}_t$, lbm/sec	Side flow, wt %	Overall mixture ratio O/F	Chamber pressure p_c, psia	Characteristic velocity c^*, ft/sec	Combustion efficiency η_{c^*}, %
		Main element $\dot{w}_{o_m}$	Side spray $\dot{w}_{o_s}$	Main element $\dot{w}_{f_m}$	Side spray $\dot{w}_{f_s}$						
1	Like	2.34	0.92	2.05	0.84	6.15	28.6	1.13	129	4095	70.3
2	Like	2.19	0.44	1.92	0.27	4.82	14.5	1.20	105	4230	73.0
3	Like	2.27	2.24	1.94	0.13	4.58	8.1	1.21	101	4297	74.1
4	None	2.29	—	1.77	—	4.06	—	1.30	91	4360	75.9
5	Unlike	2.28	0.24	1.95	0.14	4.60	8.25	1.21	108	4550	78.4
6	Unlike	2.24	0.42	1.93	0.27	4.86	14.2	1.21	117	4685	80.7
7	Unlike	2.34	0.63	2.02	0.52	5.50	20.7	1.17	131	4643	79.8
8	Unlike	2.32	0.90	2.01	0.83	6.06	28.6	1.13	142	4565	78.4

Table 5. Results of baffled-chamber firings to determine degree of stream separation of unlike impinging jets in 100-lbf injector (injector side spray)

Test No.	Kind of side spray	Oxidizer flow, lbm/sec		Fuel flow, lbm/sec		Total flow $\dot{w}_t$, lbm/sec	Side flow, wt %	Overall mixture ratio O/F	Chamber pressure p_c, psia	Characteristic velocity c^*, ft/sec	Combustion efficiency η_{c^*}, %
		Main element $\dot{w}_{o_m}$	Side spray $\dot{w}_{o_s}$	Main element $\dot{w}_{f_m}$	Side spray $\dot{w}_{f_s}$						
1	Like	0.1752	0.9538	0.1458	0.0482	0.423	24.0	1.18	106	4220	73
2	Like	0.1655	0.0295	0.1347	0.0293	0.359	15.0	1.19	94	4410	76
3	None	0.1820	—	0.1500	—	0.332	—	1.21	87	4430	76
4	Unlike	0.1650	0.0160	0.1360	0.0160	0.333	9.6	1.19	90	4560	79
5	Unlike	0.1660	0.0330	0.1370	0.0290	0.365	17.0	1.20	103	4760	82
6	Unlike	0.1720	0.0380	0.1412	0.0348	0.386	20.0	1.19	111	4880	84
7	Unlike	0.1750	0.0500	0.1400	0.0460	0.411	23.0	1.21	124	5090	88
8	Unlike	0.1750	0.0620	0.1410	0.0570	0.435	27.0	1.20	137	5330	92

Table 6. Results of baffled-chamber firings to determine degree of stream separation of unlike impinging jets in 100-lbf injector (chamber side spray)

Test No.	Kind of side spray	Oxidizer flow, lbm/sec		Fuel flow, lbm/sec		Total flow $\dot{w}_t$, lbm/sec	Side flow, wt %	Overall mixture ratio O/F	Chamber pressure p_c, psia	Characteristic velocity c^*, ft/sec	Combustion efficiency η_{c^*}, %
		Main element $\dot{w}_{o_m}$	Side spray $\dot{w}_{o_s}$	Main element $\dot{w}_{f_m}$	Side spray $\dot{w}_{f_s}$						
1	Like	0.1709	0.0291	0.1385	0.0315	0.370	16.4	1.18	94	4370	75
2	Like	0.1718	0.0222	0.1422	0.0248	0.361	13.0	1.20	94	4490	77
3	None	0.1700	—	0.1420	—	0.312	—	1.20	87	4800	80
4	None	0.1656	0.0185	0.1273	0.0143	0.328	10.7	1.30	88	4630	80
5	Unlike	0.1653	0.0297	0.1283	0.0247	0.348	16.0	1.27	99	4890	84
6	Unlike	0.1708	0.0416	0.1436	0.0350	0.391	19.6	1.19	118	5180	89
7	Unlike	0.1766	0.0524	0.1397	0.0483	0.418	24.1	1.22	128	5260	91

Table 7. Results of baffled-chamber firings to determine degree of stream separation of unlike impinging sheets in 100-lbf injector (chamber side spray)

Test No.	Kind of side spray	Oxidizer flow, lbm/sec		Fuel flow, lbm/sec		Total flow $\dot{w}_t$, lbm/sec	Side flow, wt %	Overall mixture ratio O/F	Chamber pressure p_c, psia	Characteristic velocity c*, ft/sec	Combustion efficiency η_c*, %
		Main element $\dot{w}_{o_m}$	Side spray $\dot{w}_{o_s}$	Main element $\dot{w}_{f_m}$	Side spray $\dot{w}_{f_s}$						
1	Like	0.161	0.075	0.133	0.049	0.418	29.7	1.30	108	4350	75.5
2	Like	0.160	0.036	0.133	0.035	0.369	19.2	1.17	97	4440	76.5
3	Like	0.158	0.017	0.131	0.022	0.328	11.9	1.15	95	4980	85.7
4	None	0.165	—	0.131	—	0.296	—	1.26	90	5140	89.0
5	Unlike	0.158	0.017	0.131	0.018	0.323	10.7	1.17	100	5240	90.2
6	Unlike	0.160	0.033	0.134	0.021	0.346	15.6	1.25	104	5110	88.3
7	Unlike	0.158	0.038	0.130	0.032	0.358	19.6	1.21	109	5130	88.5
8	Unlike	0.164	0.067	0.135	0.047	0.413	27.7	1.27	121	4940	85.4

Table 8. Results of baffled-chamber firings to determine degree of stream separation of unlike impinging jets in 10-lbf injector (chamber side spray)

Test No.	Kind of side spray	Oxidizer flow, lbm/sec		Fuel flow, lbm/sec		Total flow $\dot{w}_t$, lbm/sec	Side flow, wt %	Overall mixture ratio O/F	Chamber pressure p_c, psia	Characteristic velocity c*, ft/sec	Combustion efficiency η_c*, %
		Main element $\dot{w}_{o_m}$	Side spray $\dot{w}_{o_s}$	Main element $\dot{w}_{f_m}$	Side spray $\dot{w}_{f_s}$						
1	Like	0.0155	0.0036	0.0136	0.0029	0.0355	18.2	1.15	143	4920	84
2	Like	0.0171	0.0137	0.0039	0.0029	0.0372	18.2	1.24	151	4970	86
3	Like	0.0170	0.0038	0.0141	0.0030	0.0376	18.1	1.21	151	4900	84
4	Like	0.0173	0.0038	0.0143	0.0030	0.0380	18.0	1.21	151	4900	84
5	Like	0.0168	0.0025	0.0139	0.0021	0.0352	13.1	1.20	141	4920	85
6	Like	0.0171	0.0009	0.0141	0.0007	0.0324	4.9	1.19	134	5080	87
7	None	0.0173	—	0.0146	—	0.0419	—	1.19	132	5080	87
8	None	0.0167	—	0.0137	—	0.0304	—	1.22	126	5100	88
9	Unlike	0.0170	0.0009	0.0141	0.0007	0.0319	4.7	1.21	128	4910	85
10	Unlike	0.0169	0.0009	0.0138	0.0007	0.0318	4.8	1.21	127	4900	85
11	Unlike	0.0167	0.0026	0.0140	0.0021	0.0352	13.2	1.20	138	4820	83
12	Unlike	0.0168	0.0026	0.0143	0.0021	0.0354	13.0	1.20	139	4840	83
13	Unlike	0.0172	0.0038	0.0141	0.0030	0.0377	17.8	1.20	151	4910	85
14	Unlike	0.0173	0.0038	0.0142	0.0030	0.0378	17.7	1.20	151	4910	85

Table 9. Results of baffled-chamber firings to determine degree of stream separation of unlike impinging sheets in 10-lbf injector (chamber side spray)

Test No.	Kind of side spray	Oxidizer flow, lbm/sec		Fuel flow, lbm/sec		Total flow $\dot{w}_t$, lbm/sec	Side flow, wt %	Overall mixture ratio O/F	Chamber pressure p_c, psia	Characteristic velocity c*, ft/sec	Combustion efficiency η_{c^*}, %
		Main element $\dot{w}_{o_m}$	Side spray $\dot{w}_{o_s}$	Main element $\dot{w}_{f_m}$	Side spray $\dot{w}_{f_s}$						
1	Like	0.0167	0.0010	0.0140	0.0007	0.0324	5.2	1.20	129	4870	84
2	Like	0.0165	0.0027	0.0138	0.0022	0.0352	13.9	1.20	137	4750	82
3	Like	0.0163	0.0028	0.0140	0.0022	0.0342	14.0	1.17	137	4770	82
4	Like	0.0164	0.0040	0.0139	0.0031	0.0374	18.9	1.20	143	4660	80
5	Like	0.0161	0.0039	0.0132	0.0030	0.0362	19.1	1.23	138	4650	80
6	None	0.0163	—	0.0140	—	0.0303	—	1.16	121	4900	84
7	None	0.0165	—	0.0136	—	0.0301	—	1.21	121	4930	85
8	Unlike	0.0166	0.0010	0.0140	0.0007	0.0323	5.2	1.20	122	4630	80
9	Unlike	0.0161	0.0027	0.0141	0.0022	0.0341	14.0	1.15	132	4600	79
10	Unlike	0.0161	0.0028	0.0141	0.0022	0.0352	14.1	1.16	133	4620	79

$\dot{w}_{f_s}$, respectively) divided by the total flow, or

$$\frac{\dot{w}_{o_s} + \dot{w}_{f_s}}{\dot{w}_{o_s} + \dot{w}_{o_m} + \dot{w}_{f_s} + \dot{w}_{f_m}} \times 100$$

while the overall mixture ratio r is based on the total flow of fuel and oxidizer

$$r = \frac{\dot{w}_o}{\dot{w}_f} = \frac{\dot{w}_{o_s} + \dot{w}_{o_m}}{\dot{w}_{f_s} + \dot{w}_{f_m}}$$

where $\dot{w}_{o_m}$ and $\dot{w}_{f_m}$ are the oxidizer and fuel main elements, respectively. Characteristic velocity efficiency (η_{c^*}) was chosen as the comparative index of performance level. It is the ratio of the measured value of c^* to that theoretically attainable with one-dimensional isentropic flow and equilibrium expansion at the experimentally measured values of chamber pressure and mixture ratio. No corrections were made to η_{c^*} since these values were to be used primarily for comparative purposes.

VI. Discussion of Results

The experimental results from Ref. 3 and Tables 4 through 9 are plotted in Figs. 12 through 14. In all cases, performance efficiency changes were accompanied by changes in chamber pressure. However, over the limited range of chamber pressure spanned by these experiments, its effects on η_{c^*} are usually second-order and were, therefore, not expected to materially affect the results.

The variation of combustion efficiency with side flow is shown in Fig. 12 for the two kinds of 2000-lbf single elements. In both cases, combustion efficiency η_{c^*} dropped as the fraction of propellants introduced as like side sprays was increased. This indicates that the propellant streams had not penetrated each other and that the oxidizer-orifice side of the main injector spray was quite oxidizer-rich. Since there was little unreacted fuel on that side of the main element's spray with which the raw oxidizer from the side spray could react, performance was *lowered* by the amount of heat absorbed by the uncombined oxidizer. Similar arguments apply to the fuel-rich side. On the other hand, when unlike propellants were added as side sprays, the performance increased to a maximum of about 80% for both injectors. From this, it may be concluded that stream separation occurred under the conditions of these experiments. This is borne out by visual evidence, such as the photograph of Fig. 1b, which shows the flame produced by the 2000-lbf impinging-sheet injector with no side injection.

Stream separation was much more severe with the impinging jets, however. More than 40% of unlike propellants was required to counteract its deleterious effects, while only about 15% was required for the impinging sheets. Because of less separation with the sheets, their performance in the absence of side injection was markedly superior to that of the jets under the same conditions. A direct performance comparison is possible in this case, because both injectors were fired in identical combustion chambers.

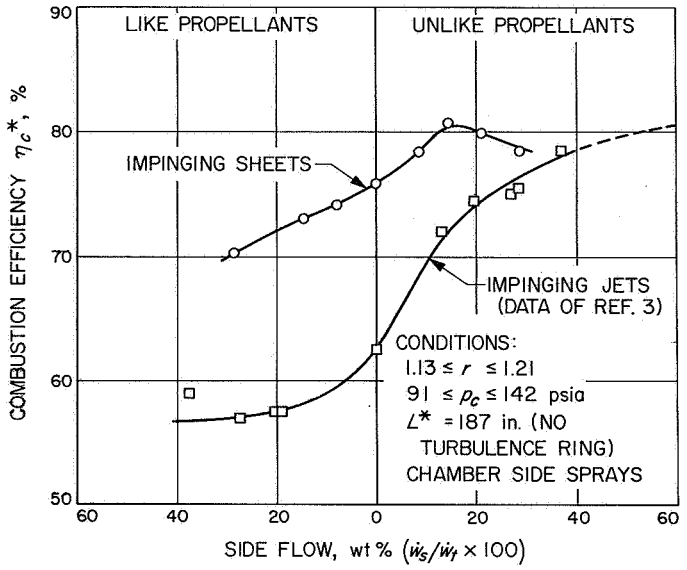

Fig. 12. Variation of combustion efficiency with side flow for 2000-lbf injector elements in identical combustion chambers

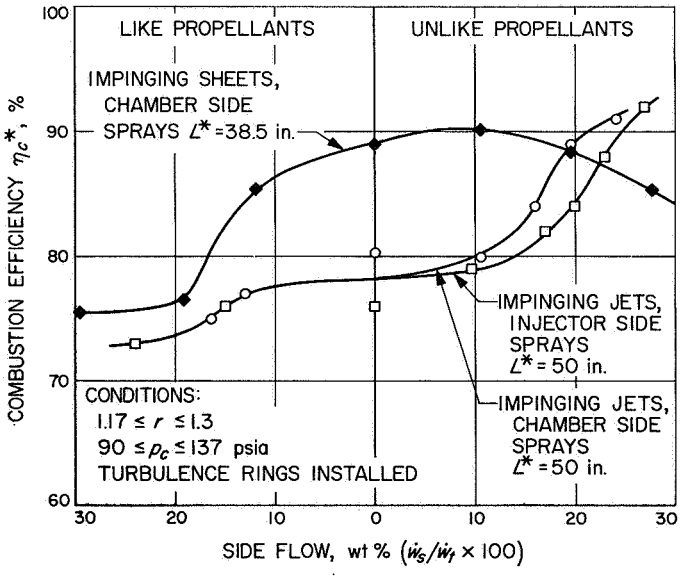

Fig. 13. Variation of combustion efficiency with side flow for 100-lbf injector elements

It should be pointed out here that the 2000-lbf impinging-sheet firings were made in a chamber without a turbulence ring. Johnson made firings in the same chamber, both with and without turbulence rings. To permit comparison on the same basis, only those of his results from Ref. 3 which were obtained *without* a turbulence ring have been plotted in Fig. 12. Not surprisingly, the additional secondary mixing of the side sprays with the separated propellant streams from the main injector

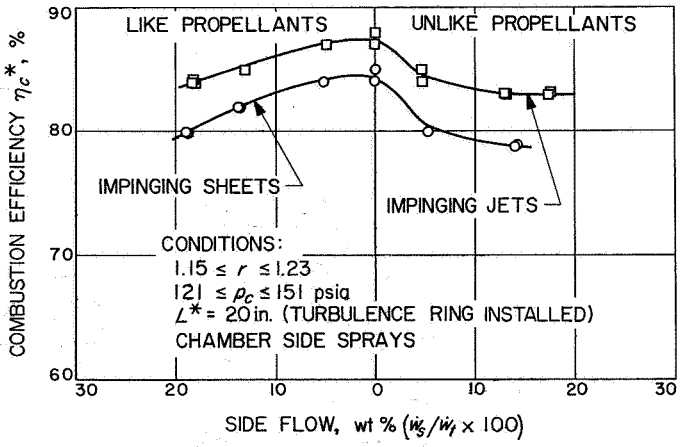

Fig. 14. Variation of combustion efficiency with side flow for 10-lbf injector elements in identical combustion chambers

induced by the turbulence devices improved performance somewhat. This indicates that a high-performance, large single element for this hypergolic propellant combination might be feasible if some attempt is made to optimize the secondary injection apparatus to promote additional mixing. Such efforts were beyond the scope or intent of the present investigation, the primary purpose of which was to detect, rather than remedy, stream separation effects.

Because of stream separation effects, one would not expect to find the same kind of mixture ratio distribution in the burning sprays from these 2000-lbf elements as is typically found (Figs. 3 and 7) under nonreactive conditions. Satisfactory correlations between cold-flow and hot-firing results are therefore not to be expected.

The variation of combustion efficiency with side flow is shown in Fig. 13 for the two kinds of 100-lbf single elements. The maximum performance ($\eta_{c^*} \cong 90\%$) with impinging sheets was realized at only about 5 to 10% side flow, and the shape of the curve indicates considerably less stream separation than was found at the 2000-lbf thrust level. Increasing the percentage of side flow, either like or unlike, lowered the performance, probably by the amount of heat absorbed by the uncombined propellant. Thus, at this thrust level practically no stream separation was observed with impinging sheets. Figure 1c, which shows no color striations in the flame from the 100-lbf impinging-sheet injector in the absence of side flows, helps substantiate that conclusion.

This behavior may be contrasted to that of the impinging jets, where performance increased by over twelve

percentage points at 25%-unlike side spray, indicating that the main element's propellant streams were still separating, although somewhat less severely than they did in the 2000-lbf jet injector. It would seem, then, that while rapid interfacial chemical reactions at the impingement interface interfere considerably with the efficient mixing of a pair of round jets at the 100-lbf thrust level, their effects can be virtually eliminated by transforming those jets into thin, flat sheets prior to impingement.

One would *still* not expect to find the same kind of mixture ratio distributions under both reactive and nonreactive conditions, however. Figures 3 and 7 show that the nonreactive sprays are characterized by stream *penetration,* whereas this did not occur with either the impinging jets or the impinging sheets at the 100-lbf thrust level.

Figure 13 also illustrates that there is basically little difference between chamber and injector locations for the side sprays. Slightly higher performance was realized with the side sprays located in the chamber.

The variation of combustion efficiency with side flow is shown in Fig. 14 for the two kinds of 10-lbf single elements. Maximum performance in both cases is realized without side spray and falls off when either like or unlike propellants are injected into the chamber. This indicates the absence of stream separation; rapid liquid-phase reactions apparently do not disrupt the impingement process when streams of this scale are used.

The decrease in performance is, however, less when *like* propellants are introduced, which indicates that some degree of penetration takes place with streams of small cross section. Mixture ratio distributions in such burning sprays would, therefore, be expected to more closely resemble those measured under nonreactive conditions.

Figure 14 shows a somewhat better performance with impinging jets than with impinging sheets. This is probably due to less efficient mixing in this particular sheet element. In the absence of combustion effects, the primary liquid-phase mixing of a pair of impinging sheets from a 25-lbf single element was found to depend strongly on a geometrical parameter h/d. This ratio was found (Ref. 9) to be a key variable in explaining the behavior of individual sheets. The influence of h/d on the *mixing factor* E_m (Ref. 10) is shown in Fig. 15. These

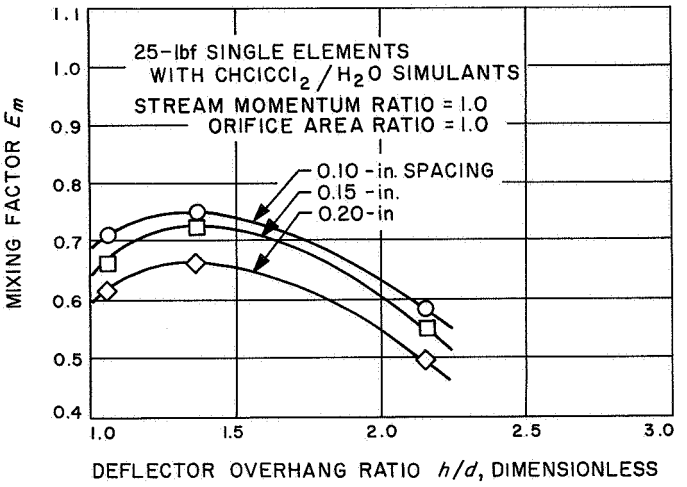

Fig. 15. Variation of mixing factor with deflector overhang ratio for single-element impinging-sheet injectors as determined from nonreactive spray tests

results indicate that, at constant deflector spacing, E_m decreases as h/d increases for $h/d \geq 1.4$. Examination of Table 2 will reveal that the 10-lbf impinging-sheet element had an h/d of 2.6, a value considerably higher than the optimum (see Fig. 15). Therefore, less efficient propellant mixing, even in the absence of stream separation, would be expected with the 10-lbf sheet injector. Had an optimized sheet element been used, the performance of both 10-lbf injectors would probably have been almost identical.

Figures 12 through 14 all show relatively low absolute performance levels; no c^* efficiency much in excess of 90% was recorded in any test. The dominant factor influencing such behavior is probably the fact that all injectors were single-element models. Even under ideal, nonreactive conditions (Figs. 3 and 7), uniform mixture ratios in the sprays from these two kinds of injectors cannot be attained. The distributions, even at best, are such that only a portion of the propellants are at the metered-in mixture ratio; the remainder burn at mixture ratios other than the optimum value. Most injectors, therefore, incorporate numbers of elements so positioned with respect to each other that additional, or secondary, mixing between adjacent spray fans can occur. It might also be expected that the performance could be atomization-limited, especially with the 2000-lbf injectors, because of the larger drop sizes produced when large streams impact each other. Atomization effects were probably negated in the present experiments, however, due to the exceedingly long chambers used, which afforded sufficient stay time for vaporization of even large propellant droplets.

The results just discussed show that, for impinging jets, stream separation effects are negligible when the diameters are small (~0.02-in.), become significant at intermediate diameters (0.06-in.), and seriously degrade performance with large (~0.25-in.) diameter jets. It thus appears that there is some critical value of a characteristic stream dimension above which disruption of the impingement process and, therefore, performance degradation, can occur. The same kind of effects were found for impinging sheets, except that they only became noticeable at larger orifice diameters. The characteristic stream dimension is, therefore, probably not the stream's cross-sectional area because, by continuity, jets and sheets formed from orifices of the same size must have the same area if frictional effects on the deflector are small.

A more meaningful correlation can be obtained if it is assumed that for jets, the characteristic dimension is their diameter, while for sheets, it is their maximum thickness, which occurs at their midpoint (Ref. 9). By use of this assumption, the results of the stream separation experiments have been compared in Table 10. It is seen that no appreciable stream separation occurred when the characteristic stream dimension was about 0.02 in. or less, but that values in excess of about 0.05 in. resulted in separation. The point of incipient combustion effects must be located somewhere between those two limiting values. At present, it is not known whether the onset of stream separation is gradual or sudden after the critical dimension is exceeded.

Stream separation occurred with the 0.06-in. orifice diameter (100-lbf thrust per element) jet injector, but *not* with the 100-lbf/element sheet injector, even though the latter device had larger (0.08-in.) orifices. This is attributed to the eight-fold reduction in the characteristic stream dimension effected by flattening the jets into thin sheets. It would, therefore, be expected that a 2000-lbf single element not susceptible to these combustion effects would be possible, provided that its sheet thickness could be reduced to something on the order of 0.02 in. The general sheet thickness correlation of Ref. 9 indicates that this could be done if the overhang ratio (h/d) of the element were greater than about 4.

VII. Conclusions

This investigation has shown that streams of the highly reactive, hypergolic propellants N_2O_4 and N_2H_4 can separate, as a result of combustion effects, into fuel-rich and oxidizer-rich combustion zones when used in two different classes of unlike-impinging doublet-injection elements at relatively low chamber pressures. The resulting reduction in mixing efficiency can seriously degrade performance (measured as c^* efficiency in this report), especially in the case of single elements, where there is no opportunity for secondary mixing through interaction with the sprays of neighboring elements.

For each individual kind of unlike doublet (impinging jets or impinging sheets), the physical size (measured as the orifice diameter) has a strong influence on the degree of severity of the combustion effects. No effects are noted for very small elements, while gross mixture-ratio maldistribution occurs with large-size elements. The behavior of both kinds of element is better correlated if a *characteristic stream dimension*, rather than the orifice size, is used. For jets, this dimension is their diameter, while for sheets, it is their maximum thickness. Combustion effects were found to be significant if the characteristic stream dimension exceeded a certain critical value. This value lies somewhere between 0.02 and 0.05 in., probably closer to the latter.

Because for a given orifice diameter impinging sheets have a smaller characteristic stream dimension than impinging jets, sheets were found in the majority of cases

Table 10. Effect of element scale on stream separation for various single-element impinging-stream injectors

Element type	Thrust per element, lbf	Orifice diameter, in.	Maximum sheet thickness, in.	Characteristic stream dimension, in.	Stream separation
Impinging-jet	2000	0.24	—	0.24	Yes
Impinging-sheet	2000	0.33	0.05	0.05	Yes
Impinging-jet	100	0.06	—	0.06	Yes
Impinging-sheet	100	0.08	0.01	0.01	Slight
Impinging-jet	10	0.022	—	0.022	No
Impinging-sheet	10	0.018	0.002	0.002	No

to exhibit less stream separation and, therefore, less performance degradation, than corresponding jets. In one case (100-lbf elements), it was found possible to virtually eliminate the separation encountered with impinging jets by forming them instead into impinging sheets, which apparently reduced their characteristic stream dimension to close to the critical value.

It was found that the distribution of mixture ratio in the spray from an unlike-impinging doublet element (either sheets or jets) can be markedly different from that measured for the same injector using nonreactive propellant simulants. Even when stream separation caused by combustion effects does not occur, the interpenetration of unlike streams noted in cold-flow studies is realized to only a slight degree in the reactive environment. This would indicate that meaningful correlations between single element cold-flow and hot-firing results may be possible only for very small element sizes.

This is not to imply that this phenomenon will seriously impair the combustion efficiency of a multi-element injector if sufficient care is taken to orient the elements to take advantage of the secondary reactions of adjacent fuel- and oxidizer-rich regions of the reacting sprays. Indeed, a knowledge of this stream separation phenomenon can be used to advantage in promoting secondary combustion and in controlling boundary flow conditions.

Nomenclature

c^* characteristic exhaust velocity, ft/sec

d orifice diameter, in.

E_m mixing factor, defined in Ref. 10

G mass flux, lb/sec-in.

h deflector overhang, in., defined by Eq. (1)

p_c chamber stagnation pressure, psia

R deflector radius, in.

r mixture ratio (oxidizer/fuel), dimensionless

$\dot{w}$ flow rate, lbm/sec

θ deflector angle, deg

η efficiency, %

Subscripts

f_s fuel, side spray

f_m fuel, main element

o_s oxidizer, side spray

o_m oxidizer, main element

s side flow

t total

max maximum

References

1. Riebling, R. W., "The Current State of Impinging-Sheet Injector Technology," presented at 9th Annual Liquid Propulsion Symposium (ICRPG), St. Louis, Missouri, October 25–27, 1967.
2. Elverum, G. W. Jr., and Staudhammer, P., *The Effect of Rapid Liquid-Phase Reactions on Injector Design and Combustion in Rocket Motors,* Progress Report No. 30-4, Jet Propulsion Laboratory, Pasadena, California, August 25, 1959.
3. Johnson, B.H., *An Experimental Investigation of the Effects of Combustion on the Mixing of Highly Reactive Liquid Propellants,* Technical Report No. 32-689, Jet Propulsion Laboratory, Pasadena, California, July 15, 1965.
4. Evans, D. D., "Injector Development," *Space Programs Summary No. 37-35, Vol. IV,* p. 152, Jet Propulsion Laboratory, Pasadena, California, October 31, 1965.
5. Stanford, H. B., "Injector Development," *Space Programs Summary No. 37-31, Vol. IV,* p. 192, Jet Propulsion Laboratory, Pasadena, California, February 28, 1965.
6. Stanford, H. B., "Injector Development," *Space Programs Summary No. 37-36, Vol. IV,* p. 174, Jet Propulsion Laboratory, Pasadena, California, December 31, 1965.
7. Riebling, R. W., "Impinging-Sheet Injectors," *Space Programs Summary No. 37-44, Vol. IV,* p. 182, Jet Propulsion Laboratory, Pasadena, California, April 30, 1967.
8. Riebling, R. W., "Stream Separation Experiments," *Space Programs Summary No. 37-45, Vol. IV,* Jet Propulsion Laboratory, Pasadena, California, June 30, 1967.
9. Riebling, R. W., *The Formation and Properties of Liquid Sheets Suitable for Use in Rocket Engine Injectors,* Technical Report No. 32-1112, Jet Propulsion Laboratory, Pasadena, California, June 15, 1967.
10. Rupe, J. H., *The Liquid Phase Mixing of a Pair of Impinging Streams,* Progress Report No. 20-195, Jet Propulsion Laboratory, Pasadena, California, August 6, 1953.